ELSEVIER

Journal of Power Sources 105 (2002) 82–86

JOURNAL OF POWER SOURCES

www.elsevier.com/locate/jpowsour

Electrochemical characterization of $Li_xNi_yCo_{1-y}O_2$ electrodes in a 1 M $LiPF_6$ solution of the ethylene carbonate–diethyl carbonate

George Ting-Kuo Fey[a,*], Wen-Hsiung Yo[a], Yu-Chi Chang[b]

[a]*Department of Chemical Engineering, National Central University, Chungli 320, Taiwan, ROC*
[b]*Department of Chemical Engineering, Tamkang University, Tamsui 251, Taiwan, ROC*

Received 6 April 2001; received in revised form 27 August 2001; accepted 3 October 2001

Abstract

The electrochemical characteristics of $Li_xNi_yCo_{1-y}O_2$ ($0.5 < y < 0.9$) prepared by a co-precipitation method were reported. Slow scan cyclic voltammetry (SSCV) and electrochemical impedance spectroscopy (EIS) were used to investigate the kinetic behavior of the composite electrodes. Kinetic data such as the Tafel slope and the charge-transfer resistance were determined based on the experimental results. An equivalent circuit model was proposed to simulate the impedance spectra and gave a good data fit. The present study also demonstrated that the kinetic data were composition-sensitive to varying lithium content and nickel content in the mixed oxide electrodes.

Keywords: Lithium intercalation/deintercalation; $Li_xNi_yCo_{1-y}O_2$; EIS; SSCV; Mixed oxide cathode

1. Introduction

The development of lithium-ion battery technology has stimulated diversified areas of research on new types of lithium insertion electrode materials [1,2]. Though problems related to the lithium anode are the main concern for commercialization of rechargeable lithium batteries, attention is shifting gradually to the cathode and related problems [3].

$LiCoO_2$ is the most widely used cathode material for commercial rechargeable lithium batteries due to its advantages, which include easy preparation, high voltage, good reversibility and high theoretical specific capacity [4]. Lithiated cobalt oxide has a layered structure in which the Li^+ and Co^{3+} ions occupy alternating (1 1 1) layers of octahedral sites in a rock salt structure [5–9]. The typical reversible limit of delithiation for Li_xCoO_2 in commercial batteries is $x = 0.5$, which corresponds to a charge capacity of ~140 mA h/g. However, layered $LiCoO_2$ often suffers from structural instability and safety problems, especially when the lithium content is lower than 0.5 (i.e. $x < 0.5$) or the charge voltage exceeds 4.3 V. In order to tackle the problems associated with cost and system stability, $LiNiO_2$ has been intensively studied [10–12] and is considered a promising cathode material for rechargeable lithium batteries due to its low cost and high energy density [13]. However, it is also known for its difficulty in synthesis with consistent quality due to its tendency for non-stoichiometry and for its poor cycling performance due to its structural instability upon cycling, and has greater safety problems [14]. Hence, a Li-ion battery in which $LiNiO_2$ is used as the cathode material is not yet available commercially. Lithiated cobalt and nickel oxides are iso-structural. Therefore, the preparation of solid solutions of $Li_xNi_yCo_{1-y}O_2$ is feasible. $Li_xNi_yCo_{1-y}O_2$ mixed oxides are considered the most prospective cathode materials and have attracted much attention in recent years [11,15–20] due to the combined advantages of their parent oxides. The substitution of cobalt for nickel improves the reversibility of the intercalation process.

Banov et al. [11] studied the electrochemical characteristics of $LiNi_yCo_{1-y}O_2$ electrodes in 1 M $LiClO_4$/propylene carbonate–dimethoxyethane (1:1, v/v) solutions using the cyclic voltammetry technique. Levi et al. [20] determined the Li-ion chemical diffusion coefficient in $Li_xNi_{0.8}Co_{0.2}O_2$ electrodes in 1 M $LiAsF_6$/ethylene carbonate–dimethyl-carbonate (1:3, v/v) solutions using the slow scan cyclic voltammetry (SSCV), potentiostatic intermittent titration, and galvanostatic intermittent titration. Croce et al. [17] investigated the electronic and ionic transport properties of the $Li_xNi_{0.75}Co_{0.25}O_2$ electrodes based on electrochemical impedance spectroscopy (EIS) measurements. The electrolyte used was a 1 M $LiClO_4$/ethylene carbonate–dimethyl-carbonate

* Corresponding author. Tel.: +886-3-422-7151-4206/425-7325; fax: +886-3-425-7325.
E-mail address: gfey@cc.ncu.edu.tw (G.T.-K. Fey).

0378-7753/02/$ – see front matter
PII: S0378-7753(01)00967-3

(1:1, v/v) solution. The effects of cation mixing between nickel and lithium ions on the electrochemical lithium intercalation reaction into $Li_{1-\delta}Ni_yCo_{1-y}O_2$ electrodes in a 1 M $LiClO_4$ propylene carbonate solution have been examined by Choi et al. [16]. Levi et al. [18] studied the phase structural characteristics of $LiNi_{0.8}Co_{0.2}O_2$ electrodes in a 1 M $LiAsF_6$/ethylene carbonate–dimethyl-carbonate solution (1:3, v/v) using the SSCV and in situ XRD techniques. Recently, Chebiam et al. [21] investigated the structural stability of chemically delithiated $Li_{1-x}Ni_yCo_{1-y}O_2$ upon exposure to moderate temperatures (50–150 °C). The kinetic behavior of electrochemical intercalation has received little attention, relative to its importance in the operation of any electrochemical battery. This may be due to the difficulties to obtain reliable kinetic information from the data measured from composite-type electrodes with porous structures.

The objectives of the present study are: (1) to examine the effects of substitution of cobalt for nickel on the electrochemical characteristics of $Li_xNi_yCo_{1-y}O_2$ using a combination of SSCV and EIS techniques; (2) to investigate the effects of substitution of cobalt for nickel and lithium content on the kinetic characteristics of electrochemical intercalation into $Li_xNi_yCo_{1-y}O_2$ electrodes. We hope that these studies may lead to a better understanding about the mechanism of the electrode process at the interface between an intercalation electrode and a non-aqueous electrolyte.

2. Experimental

A $LiNi_yCo_{1-y}O_2$ ($0.5 \leqq y \leqq 0.9$) powder sample was prepared by dissolving stoichiometric amounts of $LiOH{\cdot}H_2O$, $Ni(NO_3)_2{\cdot}6H_2O$, and $Co(NO_3)_2{\cdot}6H_2O$ in deionized water, followed by mixing, filtering, and heating the precipitate at 70 °C for 15 min. The resulting precipitate sample was heated at 110 °C to evaporate the water content. The dried precipitate was ground into a fine particle size, pressed into a pellet, then heated to 800 °C in oxygen atmosphere (at a rate of 250 °C/h), and calcinated at 800 °C for 5 h. The products were examined by X-ray diffraction (Siemens, D-5000) using Cu Kα radiation. XRD patterns of $Li_xNi_yCo_{1-y}O_2$ powder samples indicate that they are single phase.

Electrochemical tests were carried out using three-electrode cells. The cathode samples were prepared by mixing $Li_xNi_yCo_{1-y}O_2$ powders with 10 wt.% acetylene black and 5 wt.% polyvinylidene fluoride (PVDF) in *n*-methyl pyrrolidone (NMP) solution. The paste mixture was spread on Al foil, followed by pressing and drying at 110 °C for 2 h. The reference electrode and counter electrode were constructed from lithium foil and a 1 M $LiPF_6$ solution (Hashimoto) in the ethylene carbonate–diethyl carbonate (EC–DEC) (1:1, v/v) solvent mixture served as an electrolyte. The electrochemical analyses were carried out using a Solartron 1287 for SSCV and a Solartron 1250 frequency response analyzer for EIS.

3. Results and discussion

3.1. X-ray diffraction studies

The diffraction patterns recorded for all the systems in a solid solution of the general formula $LiNi_yCo_{1-y}O_2$, where $y = 0.5$, 0.6, 0.7, 0.8, or 0.9, show all peaks indexable in the *R*-3*m* space group. The lattice parameters calculated for different y values in $LiNi_yCo_{1-y}O_2$ are summarized in Table 1. The lattice parameters, both a and c, show a decrease with respect to an increase in Co content, which is a characteristic feature of solid-solutions. The c/a ratio shows an increase with respect to an increase in Co content. The increase in the ratio of lattice constants (c/a), indicates that there is a preferential expansion of the lattice in the c-axis [15]. The increase in the c/a ratio is indirect evidence of the absence of cation mixing with respect to the increase in Co content. In other words, there was an observed increase in the stability of the host matrix. However, for the $LiNi_{0.6}Co_{0.4}O_2$ system, there was an observed increase in the c value, unlike other systems of solid-solutions.

3.2. Cyclic voltammetry of the $Li_xNi_yCo_{1-y}O_2$ electrode

Fig. 1 compares a family of slow scan cyclic voltammograms measured from $LiNi_yCo_{1-y}O_2$, where $y = 0.5$, 0.6, 0.7, 0.8, or 0.9, at a scan rate of 50 μV/s. Because of the very low scan rate, these curves reflect the quasi-equilibrium condition. The shape of all the curves, except for when $y = 0.9$, remains nearly constant, which suggests that partial substitution with Co exceeding a critical value stabilizes the structure of layered $LiNi_yCo_{1-y}O_2$ cathodes. These rather involved patterns reflecting the dependence of current values on the composition and the applied potential demonstrate phase transitions occurred during the course of Li deintercalation/intercalation processes [19]. The slope of the curve obtained when $y = 0.8$ is similar to the result reported by Croce et al. [17] in a 1 M $LiClO_4$/EC–DMC (1:1, v/v) electrolyte at a scan rate of 10 μV/s, but different from the results reported by Levi et al. [19] in a 1 M $LiAsF_6$/EC–DMC (1:3, v/v) electrolyte at a scan rate of 10 μV/s. It may

Table 1
Lattice parameters calculated for the different y values in $Li_xNi_{1-y}Co_yO_2$ solid solutions.

System	a (Å)	c (Å)	c/a
$Li_xNi_{0.9}Co_{0.1}O_2$	2.8728	14.1687	4.93
$Li_xNi_{0.8}Co_{0.2}O_2$	2.8649	14.1653	4.94
$Li_xNi_{0.7}Co_{0.3}O_2$	2.8598	14.1514	4.95
$Li_xNi_{0.6}Co_{0.4}O_2$	2.8552	14.2285	4.98
$Li_xNi_{0.5}Co_{0.5}O_2$	2.8504	14.1350	4.96

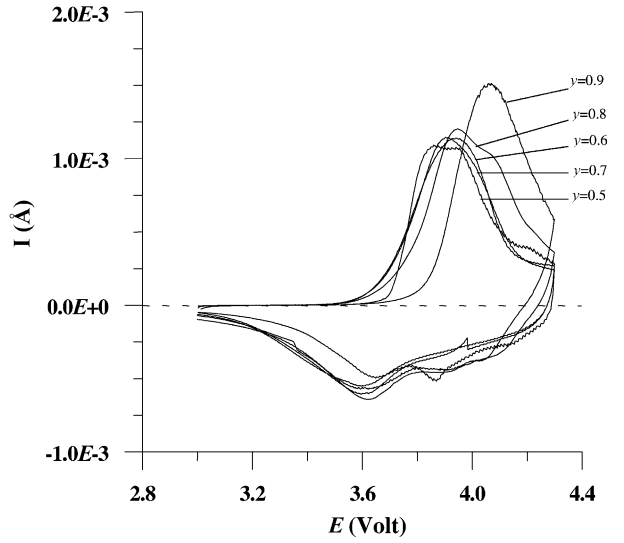

Fig. 1. Cyclic voltammograms for the $LiNi_yCo_{1-y}O_2$ for $y = 0.6$, 0.7, 0.8 and 0.9. The voltage scan rate was 0.05 mV/s. The electrolyte was 1 M $LiPF_6$/EC–DEC (1:1, v/v).

Table 2
The Tafel slopes for the Li deintercalation from $LiNi_yCo_{1-y}O_2$ where $y = 0.6$, 0.7, 0.8, 0.9[a]

$LiNi_yCo_{1-y}O_2$ (y value)	Tafel slope (mV/decade)
0.6	290
0.7	260
0.8	240
0.9	170

[a] Potential range: 3.7–3.9 V vs. Li.

also be clearly noticed that the onset of deintercalation is composition-dependent.

Levi et al. [22] have shown that at sufficiently low scan rates, the intercalation electrode's behavior is kinetically controlled. Thus, the curves shown in Fig. 1 have been used to derive the Tafel slope for Li deintercalation from Li_xNi_y-$Co_{1-y}O_2$. The results are presented in Table 2. These data show that as the nickel content of the mixed oxide electrodes increases the magnitude of the Tafel slope decreases.

3.3. Electrochemical impedance analysis

Fig. 2(a)–(c) show typical Nyquist plots obtained from $Li_xNi_{0.5}Co_{0.5}O_2$, $Li_xNi_{0.7}Co_{0.3}O_2$, and $Li_xNi_{0.9}Co_{0.1}O_2$ electrodes, respectively, at various lithium contents in a 1 M $LiPF_6$/EC–DEC (1:1, v/v) electrolyte solution. These plots were measured under open-circuit voltage conditions. The impedance spectra for these electrodes consist of two separated depressed semicircles in the high and intermediate frequency range (1–100 kHz) and a line inclined at a constant angle to the real axis in the low frequency range (<1 Hz). The two depressed semicircles are related to reactions at the interface of the electrolyte/mixed oxide electrode. The inclined line in the lower frequency range is

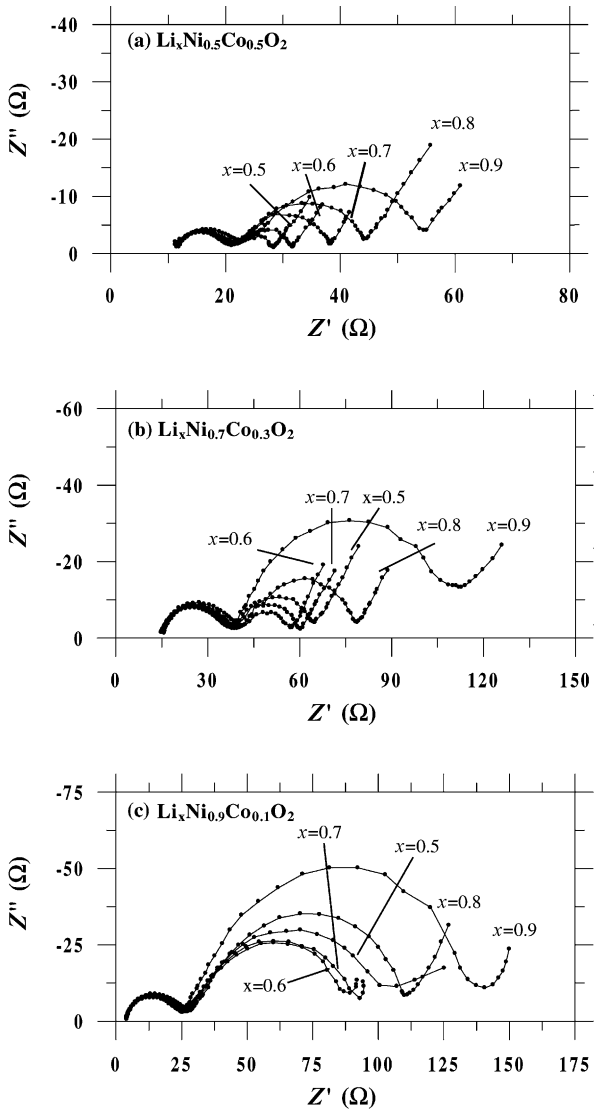

Fig. 2. Nyquist plots obtained from $Li_xNi_yCo_{1-y}O_2$ electrodes in 1 M $LiPF_6$/EC–DEC (1:1, v/v) solution as a function of lithium content: (a) $y = 0.5$, (b) $y = 0.7$, (c) $y = 0.9$.

attributable to Warburg impedance that is associated with lithium diffusion through the mixed oxide electrode [16]. It should be noted that the diameters of both the depressed high-frequency semicircle and the intermediate frequency semicircle show a characteristic dependence on lithium content, except when $x = 0.5$; the diameter increases with lithium content.

Considerable studies have been devoted to the characterization of electrochemical intercalation occurring at the interface between the intercalation electrode and the electrolyte using the EIS method [16,17,19], but there are no generally accepted equivalent circuits for lithium intercalation into porous $Li_xNi_yCo_{1-y}O_2$ electrodes. It is clear that we are still far from completely understanding their electrochemical impedance response. It has been pointed out that the intermediate frequency dispersion is characteristic of a charge-transfer process [17]. Taking this into consideration,

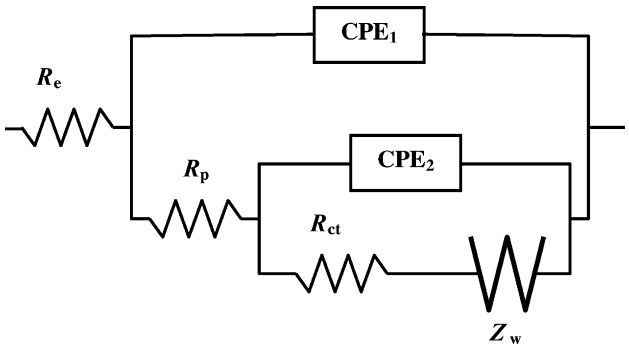

Fig. 3. Equivalent circuit used for the analysis of electrochemical intercalation of lithium into a porous $Li_xNi_yCo_{1-y}O_2$ electrode in a 1 M $LiPF_6$/EC–DEC (1:1, v/v) electrolyte. CPE_1 and CPE_2 are constant phase elements.

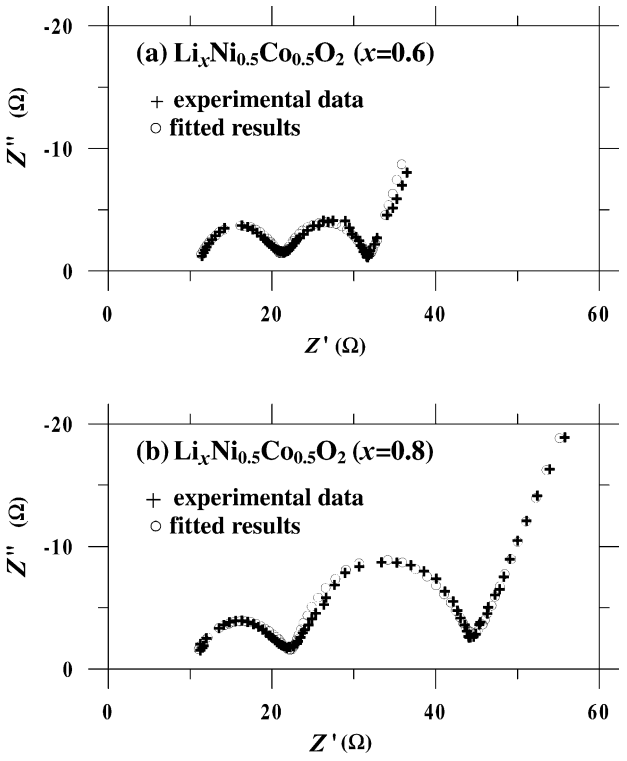

Fig. 4. Results from fitting the obtained EIS data to the proposed equivalent circuit model.

we proposed an equivalent circuit model similar to that reported by Choi et al. [16], as shown in Fig. 3. R_{ct} is the charge-transfer resistance, R_p is the resistance associated with particle-to-particle contact among the mixed oxide particles, R_e is the solution resistance, and Z_w is the Warburg impedance for diffusion of lithium ion through the mixed oxide. CPE_1 and CPE_2 are the constant phase elements which were used to describe the complicated impedance results from a porous electrode, as evidenced by the appearance of not well-defined semicircles (Fig. 2) [3].

The typical fitting results based on the proposed model are shown in Fig. 4. Table 3 summarizes the typical impedance parameters derived using the equivalent circuit (Fig. 3) for $Li_xNi_{0.8}Co_{0.2}O_2$. Taking into account the complicated nature of the response originating from a composite electrode, the agreement between the experimental and modeling data is very good. As can be seen from the table, the solution resistance is almost independent of the lithium content. The dependence of the charge-transfer resistance on lithium content is shown in Fig. 5. The charge-transfer resistance decreased as lithium content decreased. Chebiam et al. [21] showed that the lattice parameters ratio *c*/*a* increases with increased delithiation (decreasing lithium content). The decrease in diameter with respect to the increase in deintercalation level is evident from the R_{ct} values summarized in Table 3. Although the R_{ct} values show a small increase for the x values 0.6 and 0.5, there is a considerable decrease in the resistance which is attributable to the increase in electronic conductivity when compared to $x = 0.1$. In the case of the capacitance associated with the systems, there are two possible contributors, one associated with the high frequency depressed semi-circle and the other one associated with the middle frequency semicircle. The capacity associated with the high frequency semicircle is of the order of 10^{-6} F, which is typical of the capacitance associated with the surface film [22]. The capacitance associated with the middle frequency semicircle is due to the surface film/oxide particle interface, which is of several mF [22]. All the results in the present study are summarized in Table 3 and are consistent with those previously reported [17–20].

A similar trend was observed when lithium absorption resistance varied with lithium content for the porous $Li_{1-\delta}CoO_2$ electrode [23] and the composite $Li_{1-\delta}Ni_yCo_{1-y}O_2$ electrode ($y = 0.5$–1) [16]. However, the results for $Li_xNi_{0.8}Co_{0.2}O_2$ and $Li_xNi_{0.9}Co_{0.1}O_2$ are different from those

Table 3
A typical table containing the impedance parameters calculated using the model shown in Fig. 3 for $Li_xNi_{0.8}Co_{0.2}O_2$

$Li_xNi_{0.8}Co_{0.2}O_2$ (x value)	OCV (V)	R_e (Ω)	R_p (Ω)	R_{ct} (Ω)	CPE1		CPE2		Z_w		
					T × E-5 (F)	P (F)	T (F)	P (F)	R (Ω)	T (Ω)	P (Ω)
0.9	3.66	4.43	25.86	108.80	2.65	0.795	0.0077	0.828	210	1064	0.639
0.8	3.79	3.61	30.71	26.71	3.71	0.752	0.0061	0.791	131	1055	0.699
0.7	3.87	4.48	27.00	24.17	2.21	0.808	0.0063	0.777	150	1675	0.615
0.6	4.00	4.54	36.07	30.97	1.82	0.823	0.0054	0.817	189	1774	0.625
0.5	4.18	4.45	30.26	44.46	1.82	0.823	0.0068	0.765	237	1685	0.514

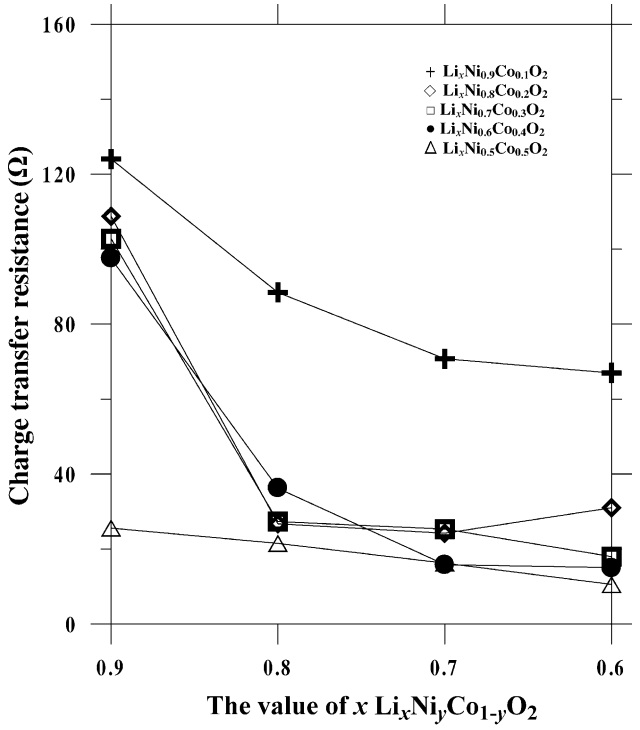

Fig. 5. The charge-transfer resistance of the intercalation reaction into $Li_xNi_yCo_{1-y}O_2$ as a function of lithium content.

reported by Choi et al. [23], which showed much lower values. Fig. 5 also indicates that charge-transfer resistance increased as nickel content in the mixed oxide increased (for electrodes with the same lithium content). These results suggest that charge-transfer resistance is composition-sensitive.

4. Conclusions

SSCV and EIS techniques have been used to investigate $Li_xNi_yCo_{1-y}O_2$ electrodes. An equivalent circuit model has been proposed to simulate the impedance spectra, which fits well with the experimental results.

The results obtained in this study demonstrate that the Tafel slope and charge-transfer resistance for the electrochemical lithium intercalation/deintercalation reactions into/from composite $Li_xNi_yCo_{1-y}O_2$ electrodes in a 1 M $LiPF_6$/EC–DEC (1:1, v/v) solution can be plotted as functions of lithium and nickel content. The Tafel slope decreases as nickel content increases. The charge transfer resistance, when $y = 0.5$–0.9, increases with increasing lithium and nickel content.

Acknowledgements

This work was supported by the National Science Council of the Republic of China, under Contract no. NSC-90-2214-E-008-003. The authors would also like to thank Dr. V. Subramanian for his help and insight in this work.

References

[1] D. Aurbach, M.D. Levi, E. Levi, H. Teller, B. Markovsky, G. Salitra, U. Heider, L. Heider, J. Electrochem. Soc. 145 (1998) 3024.
[2] S. Panero, P. Reale, F. Bonino, B. Scrosati, M. Arrabito, S. Bodoardo, D. Mazza, N. Penazzi, Solid State Ionics 128 (2000) 43.
[3] J. Fan, P.S. Fedkiw, J. Power Sources 72 (1998) 165.
[4] T. Nagaura, K. Tazawa, Prog. Batteries Solar Cells 9 (1990) 20.
[5] L.D. Dyer, B.S. Borie Jr., G.P. Smith, J. Am. Chem. Soc. 76 (1954) 1499.
[6] W.D. Johnston, R.R. Heikes, D. Sestrich, J. Phys. Chem. Solids 7 (1958) 1.
[7] K. Mizushima, P.C. Jones, P.J. Wiseman, J.B. Goodenough, Mater. Res. Bull. 15 (1980) 783.
[8] H.J. Orman, P.J. Wiseman, Acta Cryst. C 40 (1984) 12.
[9] T.A. Hewston, B.L. Chamberland, J. Phys. Chem. Solids 48 (1987) 97.
[10] Y.-M. Choi, S.-I. Pyun, J.-S. Bae, S.-I. Moon, J. Power Sources 56 (1995) 25.
[11] B. Banov, J. Bourilkov, M. Mladenov, J. Power Sources 54 (1995) 268.
[12] Y.-M. Choi, S.-I. Pyun, S.-I. Moon, Y.-E. Hyung, J. Power Sources 72 (1998) 83.
[13] S. Megahed, W. Ebner, J. Power Sources 54 (1995) 155.
[14] J.R. Dahn, E.W. Fuller, M. Obrovac, U. von Sacken, Solid State Ionics 69 (1994) 265.
[15] J. Cho, H.-S. Jung, Y.-C. Park, G. Kim, H.S. Lim, J. Electrochem. Soc. 147 (2000) 15.
[16] Y.-M. Choi, S.-I. Pyun, S.-I. Moon, Solid State Ionics 89 (1996) 43.
[17] F. Croce, F. Nobili, A. Deptula, W. Lada, R. Tossici, A. D'Epifanio, B. Scrosati, R. Marassi, Electrochem. Commun. 1 (1999) 605.
[18] E. Levi, M.D. Levi, G. Salitra, D. Aurbach, R. Oesten, U. Heider, L. Heider, Solid State Ionics 126 (1999) 97.
[19] M.D. Levi, K. Gamolsky, D. Aurbach, U. Heider, R. Oesten, Electrochim. Acta 45 (2000) 1781.
[20] M.D. Levi, K. Gamolsky, D. Aurbach, U. Heider, R. Oesten, J. Electroanal. Chem. 477 (1999) 32.
[21] R.V. Chebiam, F. Prado, A. Manthiram, J. Electrochem. Soc. 148 (2001) A49.
[22] M.D. Levi, G. Salitra, B. Markovsky, H. Teller, D. Aurbach, U. Heider, L. Heider, J. Electrochem. Soc. 146 (1999) 1279.
[23] Y.-M. Choi, S.-I. Pyun, Solid State Ionics 99 (1997) 173.